Institute of Physics Publishing
doi:10.1088/1742-6596/32/1/065
Journal of Physics: Conference Series **32** (2006) 424–431
Sixth Edoardo Amaldi Conference on Gravitational Waves

Downselect of the signal extraction scheme for LCGT

K. Kokeyama[1], S. Sato[2], F. Kawazoe[1], K. Somiya [3], M. Fukushima [2], S. Kawamura[2], Akio Sugamoto[4]

[1] The Graduate School of Humanities and Sciences, Ochanomizu University, 2-1-1, Otsuka, Bunkyo-ku, Tokyo, 112-8610 Japan
[2] TAMA project, National Astronomical Observatory of Japan
2-21-1, Osawa, Mitaka, Tokyo 181-8588 Japan
[3] Max-Planck-Institut für Gravitationsphysik, Am Mühlenberg 1, 14476 Potsdam, Germany
[4] Ochanomizu University, 2-1-1, Otsuka, Bunkyo-ku, Tokyo, 112-8610 Japan

E-mail: keiko.kokeyama@nao.ac.jp

Abstract. Large Cryogenic Gravitational wave Telescope (LCGT) is the future Japanese gravitational-wave detector. It will employ the broadband resonant sideband extraction (RSE) as its optical configuration. We compared four signal extraction schemes that have been proposed so as to downselect one of them as the scheme for LCGT. The selected scheme uses the phase and amplitude modulation sidebands: the phase modulation sidebands transmitting to the antisymmetric port (AP) and the amplitude modulation sidebands reflected to the symmetric port (SP) by the functions of the Michelson asymmetry. Using these sidebands, a new technique called 'delocation' is applicable. One advantage is that the control signals of the undesired signals do not appear at the AP, where the differential signals appear.

.

1. Introduction

Large Cryogenic Gravitational wave Telescope (LCGT) is the future Japanese gravitational wave (GW) detector. Various new techniques, such as a very high power laser, an advanced suspension system, the cryogenics, and a new optical configuration will be applied in order to establish the new GW astronomy. As for the optical configuration, the resonant sideband extraction (RSE) is selected as the optical design of LCGT. There have been several prototype experiments to demonstrate the RSE interferometer especially for the Advanced LIGO which is the US future GW detector [3] [4] [5] [6].

The topology of the RSE interferometer is shown in Figure 1. Fabry-Perot (FP) arm cavities are placed to enhance the GW signals. The power-recycling mirror (PRM) reinjects the light reflected the Michelson interferometer (MI) to increase the effective laser power for the better shot noise. In addition, there is the signal extraction mirror (SEM) at the antisymmetric port (AP). It reduces the effective finesse of the arm cavities for the GW signals. The signals can be extracted before over-circulating in the FP cavities. Therefore the SEM improves the sensitivity of the interferometer at higher frequencies. On the other hand, since the carrier light returns to the symmetric port (SP), the SEM at the AP does not affect the light power inside the arm cavities. The MI can be regarded as a compound mirror with its reflectivity $r_{\mathbf{MI}}$. It is determined by choosing the MI asymmetry length Δl and the sideband frequency ω. The reflectivity approximately satisfies $r_{\mathrm{MI}} = \cos\alpha$, where $\alpha = \frac{\Delta l \omega}{c}$.

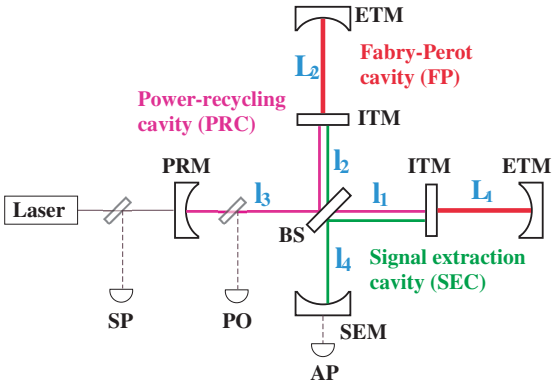

Figure 1. Optical configuration of the RSE interferometer. The two FP cavity lengths are L_1 and L_2. The MI has two light paths whose lengths are l_1 and l_2. l_3 is the distance from the PRM to the BS, and l_4 is the path length from the BS to the SEM. A power-recycling cavity (PRC) is a compound cavity which is completed by the PRM and the MI. A signal extraction cavity (SEC) is also a compound cavity, formed by the MI and SEM. There are three signal detection ports, a symmetric port (SP), an antisymmetric port (AP) and a pick-off port (PO).

The interferometer consists of four cavities and a Michelson interferometer. These are five degrees of freedom to be controlled: the arm common mode L_+, the arm differential mode L_-, the PRC length l_+, the MI differential length l_-, the SEC length l_s. They are defined in Table 1. They have to be controlled properly to operate the interferometer. Therefore we must extract the five signals of the longitudinal degrees of freedom. To select the signal extraction scheme for LCGT we have studied and compared the four schemes, which was proposed or partially tested by the tabletop experiments.

In the next section, the basic concepts and techniques of signal extraction will be explained. In Section 3, the four signal extraction schemes will be reviewed. In Section 4, we will compare these schemes to downselect one as the LCGT design. In Section 5, we will present the conclusion.

Description	Symbol	the length
Common length of the arm cavities	L_+	$L_1 + L_2$
Differential length of the arm cavities	L_-	$L_1 - L_2$
PRC length	l_+	$l_3 + \bar{l}$
Differential length of the MI	l_-	$l_1 - l_2$
SEC length	l_s	$l_4 + \bar{l}$

Table 1. Five longitudinal degrees of freedom in the interferometer. L_1 and L_2 are the lengths of the inline and perpendicular FP cavities, respectively. l_1 and l_2 designate the inline and perpendicular path lengths of the MI. $\bar{l} = (l_1 + l_2)/2$ is the average of the light path length of the MI. l_3 and l_4 denote the distance from the PRM to the BS, and from the BS to the SEM. They are also shown in Figure 1.

2. Fundamental concepts of signal extraction

To control the interferometer, the length sensing system is indispensable for the feedback control. An important point of sensing is how to get the proper signals of all longitudinal degrees of freedom.

We need the carrier light together with two sets of sidebands to extract the five kinds of signals. The L_+ and L_- signals are obtained from the beat between the carrier and a set of phase modulation (PM) sidebands (demodulation, DM). They are relatively independent from the other control signals, being accumulated in the high-finesse FP cavities. The difficulty

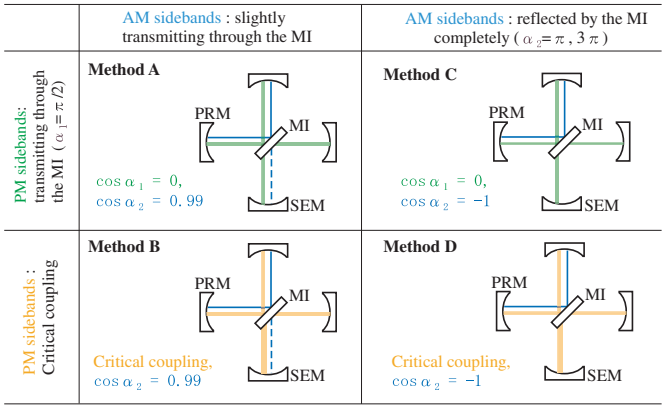

Figure 2. Comparison of the four methods. The PM sidebands go into the SEC mostly or completely to carry the l_s signal. Almost or all the AM sidebands do not go into the SEC, avoiding cross-coupling of the l_+ and l_s signals.

is that the l_+, l_- and l_s signals are overwhelmed by the enhanced L_+ and L_- signals. The straightforward solution is to utilize two sets of sidebands which do not go into arm cavities and to extract the three signals by beating between the two sidebands (double demodulation, DDM [7]). We prepare the carrier, a set of PM sidebands and a set of amplitude modulation (AM) sidebands. The PM sidebands works as a local oscillator to extract the L_+ and L_- signals at the SP and AP relatively. This is the same as a control scheme of the FP Michelson interferometer. Beating between the PM and AM sidebands gives the l_+, l_- and l_s signals by the double demodulation technique, where one of the sidebands works as a probe and the other as a local oscillator. It requires that the second sidebands must be the AM sidebands so that a non-zero signal can be produced by beating between with the PM sidebands. The PM and AM sidebands must be at different RF frequencies since the detected signals must not be at zero frequency.

3. Four control methods

The key points of the four control methods are how to set the resonant conditions of the two sidebands, and how to determine the MI asymmetry length. With respect to these points, the four signal extraction methods will be reviewed in this section.

3.1. Method A

'Method A' is the extended version of the Advanced LIGO scheme designed by the LIGO group [8]. The conditions are: the PM sidebands completely transmitting the MI and most of the AM sidebands reflected by the MI. The PM sidebands have to resonate in both of the PRC and the SEC, and the AM sidebands have to resonate only in the PRC (upper left of Figure 2). Actual Advanced LIGO will employ the detuned RSE configuration and will use two sets of PM sidebands.

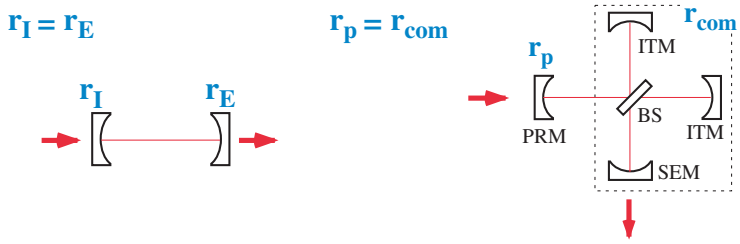

Figure 3. Conceptual drawing of critical coupling. When the reflectivities of the front mirror and the end mirror are equal ($r_{\mathrm{I}} = r_{\mathrm{E}}$), all the light fields pass through the cavity. For the RSE interferometer, the PRM corresponds to the front mirror and the compound mirror completed by the MI and the SEM corresponds to the end mirror. When their reflectivities satisfy $r_{\mathrm{p}} = r_{\mathrm{com}}$, the light fields go through to the AP.

Table 2 represents the sensing matrix of method A. The sensing matrix was calculated by the software FINESSE [13]. In the sensing matrix, the desired signal components are set to unity by normalized factors (norm) and the signal values less than 1e-5 are considered to be 0.

3.2. Method B

'Method B' was developed by Somiya and has been partially tested with a Japanese prototype experiment [9]. A combination of the MI asymmetry length and the PM sideband frequency is set as the 'critical coupling' condition for the PM sidebands. Considering a simple cavity of two mirrors, the critical coupling requires that the both mirrors have same reflectivities and the cavity satisfies the resonant condition. To apply to the interferometer, the reflectivity of the PRM and the compound reflectivity of the MI and the SEM have to be the same (Figure 3). In this condition, the PM sidebands are maximized inside the SEC and all the light fields pass through the SEM. Thus, it has the maximum sensitivity to the l_s signal. The AM sidebands slightly reach the SEM as well as method A (lower left of Figure 2). In this method, the low frequency sidebands and short asymmetry lengths are available.

Table 3 represents the sensing matrix of method B. The L_+ signal is extracted at the PO because the amount of the local oscillator (the PM sideband) is small at the SP under the critical coupling condition.

3.3. Method C

'Method C' was developed in combination with the double demodulation by Sato [10]. Keywords are $\cos\alpha_1 = 0$ and $\cos\alpha_2 = -1$ [11], where $\alpha_1 =$ and $\cos\alpha_2$ denote the MI reflectivities for the PM sidebands and the AM sidebands respectively. With the help of these reflectivities, the PM sidebands pass through the MI completely, and the AM sidebands are completely reflected by

the MI (upper right of Figure 2) [1]. Table 4 represents the sensing matrix under this condition.

The light fields at the PO with the demodulation phases chosen to extract the l_+ or l_s signals at its maximum strengths contain both of the two components. However, with a new technique called 'delocation' [10], these signals can be perfectly isolated from each other. The delocation is detuning of the AM sidebands by displacing the PRM. It can change the resonant condition of the AM sidebands in the PRC and the off-resonance AM sidebands can rotate the optimal demodulation phases of these signals [2]. The demodulation phase to maximize the l_+ signal can be rotated by $\pi/2$ from that to maximize the l_s signal with an appropriate amount of the delocation. Thus the two signals can be extracted optically cleanly by choosing the respective demodulation phases. This scheme can not be applied to neither A nor B methods because the AM sidebands enter the SEC and the phase of the l_s signal has been already rotated.

When the delocation is applied, the coupling between the five kinds of signals is relatively small (Table 5). We call this condition the diagonalization of the signals, with which the robust control of the interferometer is expected. Although, the signals extracted by the other three methods are also orthogonal and can be separated by the signal calculation processes, they have potential risks to contaminate the extracted signals during those processes, such as noise injection. Therefore the optically diagonalized signals are considered to be advantageous in many aspects.

3.4. Method D

In 'method D' [12], the combination of the MI asymmetry length and the PM sideband frequency is set as the critical coupling condition by the same way of method B. The PM sidebands are maximized in the SEC and reach the SEM. For the AM sidebands, the MI reflectivity is $r_{MI} = \cos\alpha_2 = -1$ to make the AM sidebands reflected by the MI completely. Table 6 represents the sensing matrix under this condition. The delocation is also applicable (lower right of Figure 2). Table 7 represents the sensing matrix when the delocation is applied.

4. Downselect of four methods for the LCGT

Method C was chosen as the signal extraction scheme for LCGT, based on the following considerations. The delocation was not adopted at the present moment because there is little experience with this technique. A present plan is to diagonalize the signals by the signal calculation processes of the extracted signals. However it is important that there is still a possibility of expanding to the optical diagonalization of signals.

4.1. Difficulty of setting parameters

One problem of methods B and D is that the number of the parameter sets which can realize the methods is limited, because of the strong constraint between the parameters. To determine the PM, AM sideband frequencies and the MI asymmetry length, (1) the sidebands should resonate in the mode-cleaner placed before the interferometer, (2) The PM sideband frequency and the MI asymmetry length should be determined so that $r_{\rm p} = r_{\rm com}$ is satisfied, where $r_{\rm com} = -r_{\rm MI} + (t_{\rm MI}^2\, r_{\rm s})/(1 - r_{\rm MI}\, r_{\rm s})$ for the critical coupling condition, and (3) the AM sideband frequency is determined automatically depending on the MI asymmetry lengths, however, the PM and AM sideband frequencies must have at least one common divisor because both of them should be resonate in the common cavity, the PRC.

[1] The sideband conditions of [10] and [11] methods are similar, however, they are based on a different concept and different demodulation technique.

[2] The SEM should be moved by the same amount as the PRM is moved to keep the PM sidebands resonant. The power of the PM sidebands should not be reduced in the PRC and SEC to work as a local oscillator for the GW signal.

		L_+	L_-	l_+	l_-	l_s	norm.
SP	DM	1	0	-2.50e-3	0	1.27e-3	10.8
AP	DM	0	1	0	1.25e-3	0	5.95
SP	DDM	-1.90e-3	0	1	-2.73e-4	-0.505	0.0063
AP	DDM	0	1.26e-3	1.37e-3	1	3.63e-4	0.00150
PO	DDM	-8.35e-4	0	1.66	5.96e-4	1	0.0218

Table 2. Sensing matrix of method A.

		L_+	L_-	l_+	l_-	l_s	norm.
PO	DM	1	0	-6.54e-4	0	5.45e-4	216
AP	DM	0	1	0	1.25e-3	0	13.0
SP	DDM	-5.69e-4	-1.57e-5	1	-1.13e-2	0.596	0.00554
AP	DDM	0	1.39e-3	0	1	0	0.00155
PO	DDM	3.63e-3	-5.20e-4	-1.62	0	1	0.0225

Table 3. Sensing matrix of method B

		L_+	L_-	l_+	l_-	l_s	norm.
SP	DM	1	0	-2.55e-3	0	1.29e-3	13.4
AP	DM	0	1	0	1.25e-3	0	6.62
SP	DDM	-2.14e-3	0	1	5.96e-4	-0.505	0.0064
AP	DDM	0	2.89e-3	0	1	0	0.00151
PO	DDM	-1.94e-3	0	1.65	-1.18e-3	1	0.0220

Table 4. Sensing matrix of method C

		L_+	L_-	l_+	l_-	l_s	norm.
SP	DM	1	0	-2.56e-3	-6.19e-5	-1.29e-3	13.4
AP	DM	0	1	0	1.25e-3	0	6.62
PO	DDM	-1.70e-3	0	1	0	0	0.0210
AP	DDM	0	1.70e-3	0	1	0	0.00103
PO	DDM	8.79e-4	0	0	0	1	0.0149

Table 5. Sensing matrix of method C with the delocation.

Furthermore, they must fit the LCGT design. LCGT design parameters such as cavity lengths and mirror reflectivities are already planned roughly, so the parameters must be within the limits.

Considering these situations, there are a few parameter candidates for method B. In method D, it is very difficult to find the solution so that the AM sideband frequency may exactly satisfy $\cos\alpha_2 = \cos(\Delta l\ \omega_2/c) = -1$ within the limit of the realizable parameters (in fact, there is only one parameter set for LCGT). Methods A and C have similar steps to determine the parameters. However, in the step (3), the AM frequency parameters are always available. They have always common devisors, because for example of method C, the PM and AM sideband frequencies satisfy $\Delta l\omega_1/c = \pi/2$ and $\Delta l\omega_2/c = 3\pi$ respectively.

		L_+	L_-	l_+	l_-	l_s	norm
PO	DM	1	0	-6.56e-4	-6.32e-4	4.31e-4	290
AP	DM	0	1	0	1.25e-3	0	14.3
SP	DDM	-3.64e-4	0	1	-1.04e-3	0.713	0.00467
AP	DDM	0	1.25e-3	0	1	0	0.00514
PO	DDM	3.28e-3	0	-1.62	-1.46e-3	1	0.0226

Table 6. Sensing matrix of method D

		L_+	L_-	l_+	l_-	l_s	norm.
PO	DM	1	0	-6.56e-4	4.94e-5	-4.36e-4	290
AP	DM	0	1	0	1.25e-3	0	14.3
PO	DDM	-1.26e-3	0	1	0	0	0.0267
AP	DDM	0	1.25e-3	0	1	0	0.00223
PO	DDM	1.26e-3	0	0	0	1	0.0165

Table 7. Sensing matrix of method D with the delocation.

4.2. Diagonalized signals

The optically diagonalized signals can be extracted by methods C and D using the delocation scheme. As we explained in section 3.3, the diagonalized signals will realize the simple and robust control system because the signals have information of mostly one degree of freedom and can be used for feedback directly. However, the signal values are reduced since the power in the PRC is reduced by the displacement of the PRM. It is necessary to test this new scheme practically before applying the idea.

4.3. Clean l_- signal

The AM sidebands reflected by the MI completely can carry the clean l_- signal to the AP even when there are some imperfections or when the delocation is applied. The l_- signal has to be high quality since it appears in the L_- signal at the same signal extraction port (AP, see the matrices). The fluctuation of the l_- signal may limit the sensitivity for the GWs. The AP is the most appropriate signal detection port for the l_- signal because it has the better signal-to-noise ratio. The AM sideband condition of methods C and D can realize this completely clean l_- signal. In this condition, the l_- signal extracted from the AP is completely free from the mixture of the other two, the l_+ and l_s signals.

4.4. Summary

Considering all these factors together, method C has been chosen as the signal extraction scheme for LCGT. It can also become the back-up scheme for Advanced-LIGO. The other good point of this method is that the way to use the sidebands is very simple. Our comparison of the four methods is shown in Table 2.

5. Conclusion

We introduced and compared the four signal extraction schemes for the RSE interferometer. The four methods are distinguished by the sideband conditions and the function of the MI asymmetry. In consequence, method C was proposed for LCGT. The selected scheme has an extensibility to apply the delocation technique and the optically diagonalized signals can be

method	parameter choice	the delocation	l_-
A	many	N/A	clean
B	a few	N/A	clean
C	many	applicable	clean with the delocation
D	difficult	applicable	clean with the delocation

Table 8. Summary of our discussion. Methods B and D have a few realizable parameters. The delocation is applicable to methods C and D. The perfect clean l_- signal can be taken by methods C and D even when the delocation is applied.

expected. In addition, the clean l_- signal can be taken at the AP. The prototype experiment is planned to demonstrate the scheme including the delocation technique at National Astronomical observatory of Japan.

Acknowledgments
We wish to acknowledge a Grant-in-Aid for Scientific Research on Priority Areas (415) of the Ministry of Education, Culture, Sports, Science and Technology.

[1] K. Kuroda *et al*, *International Journal of Modern Physics D*, Vol. 8, No.5 (1999) 557-579
[2] J. Mizuno, K. A. Strain, P.G. Nelson, J. M. Chen, R. Schilling, A. Rüdiger, W. Winkler and Danzmann, 1993 *Phys. Lett. A* **175** 273-76
[3] K. A. Strain *et al*, 2003 *Appl. Opt.* **42** 1244-1256
[4] J. E. Mason and P. A. Willems 2003 *Appl. Opt.* **42** 1269-1282
[5] G. Müller, T. Delker, D. B. Tanner, D. Reitze 2003 *Appl. Opt.* **42** 1257-1268
[6] D. A. Shaddock, M. B. Gray, C. Mow-Lowry, and D. E. McClelland, 2003 *Appl. Opt.* **42** 1283-1295
[7] K. A. Strain *et al*, 2003 *Appl. Opt.* **42** 1244-1256
[8] J. E. Mason and P. A. Willems 2003 *Appl. Opt.* **42** 1269-1282
[9] K. Somiya *et al*, 2005 *Appl. Opt.* **44** 3179-3191
[10] S. Sato *et al*, in this volume
[11] G. Müller, T. Delker, D. B. Tanner, D. Reitze 2003 *Appl. Opt.* **42** 1257-1268
[12] K. Kokeyama *et al*, in preparation
[13] http://www.rzg.mpg.de/ adf/